Kapal: Jurnal Ilmu Pengetahuan dan Teknologi Kelautan
(Kapal: Journal of Marine Science and Technology)
journal homepage : http://ejournal.undip.ac.id/index.php/kapal
2301-9069 (e)
1829-8370 (p)

Transmission Coefficient Analysis of Notched Shape Floating Breakwater Using Volume of Fluid Method: A Numerical Study

Asfarur Ridlwan[1) *)], Haryo Dwito Armono[2)], Shade Rahmawati[2)], Tuswan[3)]

[1)] Department of Ocean Engineering, Institut Teknologi Sumatera, South Lampung 35365, Indonesia
[2)] Department of Ocean Engineering, Faculty of Marine Technology, Institut Teknologi Sepuluh Nopember, Surabaya 60111, Indonesia
[3)] Department of Naval Architecture, Faculty of Marine Technology, Institut Teknologi Sepuluh Nopember, Surabaya 60111, Indonesia
[*)] Corresponding Author : asfarur.ridlwan@kl.itera.ac.id

Article Info

Keywords:
CFD,
Floating breakwaters,
Transmission coefficient,
Volume of fluid

Article history:
Received: 13/12/20
Last revised: 29/01/21
Accepted: 03/02/21
Available online: 03/02/21
Published: 28/02/21

DOI:
https://doi.org/10.14710/kapal.v18i1.34964

Abstract

As one of the coastal structures, breakwaters are built to protect the coastal area against waves. The current application of breakwaters is usually conventional breakwaters, such as the rubble mound type. Climate change, which causes tidal variations, sea level height, and unsuitable soil conditions that cause large structural loads, can be solved more economically by employing floating breakwater. In this study, numerical simulations will be conducted by exploring the optimum floating breakwater notched shapes from the Christensen experiment. The comparison of three proposed floating breakwater models, such as square notch (SQ), circular notch (CN), and triangular notch (VN), is compared with standard pontoon (RG) to optimize the transmission coefficient value is analyzed. Numerical simulations are conducted using Computational Fluid Dynamics (CFD) based on the VOF method with Flow 3D Software. Compared to the experimental study, the RG model's validation shows a good result with an error rate of 8.5%. The comparative results of the floating breakwater models are found that the smaller the transmission coefficient value, the more optimal the model. The SQ structure has the smallest transmission coefficient of 0.6248. It can be summarized that the SQ model is the most optimal floating breakwater structure.

1. Introduction

The breakwater is one of the coastal structures designed to protect ships, marine ecosystems, port facilities, and coastal protection against waves. The conventional breakwater is generally applied in shallow water, and its geometry is a bottom-founded structure. The unconventional breakwater is known as the floating breakwater for deep water. It is found that there are several advantages of the floating breakwater, such as more environmentally friendly to pollution and sedimentation problems because it does not inhibit water circulation [1] and easy to relocate to another location [2]. When seawater level (SWL) rises due to tides or climate change, floating breakwater can adjust, which is more economical than a bottom-founded structure. Further, floating breakwater may be the only solution for high load structures to poor soil conditions [3].

Scientists and engineers did a tremendous development of floating breakwater research either experimentally, numerically, or a combination of both. Most research has usually been conducted to analyze various geometric shapes, configurations, or bilge keels of the floating breakwater on the wave characteristics. Recently, the interest in both numerical and experimental studies of floating breakwaters is increasing. Christensen and Bingham [2] conducted physical experiments and numerical modeling to evaluate transmission, reflection, and performances of regular pontoon (RG), wing plate (WP), and porous media (WP-P100). The study showed that wing plates (WP) reduced the floating breakwater motions, while WP and (WP-P100) reduced the refection and transmission more effectively. An experimental study for a dual rectangular pontoon floating breakwater with two treatments (single-row and double-row) is conducted by [4]. The result indicated that double-row floating breakwater significantly reduced transmission, especially for short-period waves, compared to the single-row floating breakwater.

Moreover, Cho [5] investigated the transmission of incident waves interacting with vertical porous side plates using the matched eigenfunction expansion method (MEEM). Wang and Sun [6] conducted an experimental study of a porous floating breakwater with large fabricated numbers of diamond-shaped blocks to reduce transmitted wave height and mooring force. Furthermore, the review by [7], [8], [9] conducted an experimental new type of floating breakwater. The result showed that a new type of floating breakwater's transmission coefficient had better than the traditional regular pontoon. A numerical

study of a single pontoon floating breakwater to estimate the nonlinear dynamics using the volume of fluid (VOF) method is investigated in [10]. Lastly, a numerical simulation of wave overtopping performance above caisson breakwaters utilizing the VOF method is reviewed [11]. The hydrodynamics performance of cylindrical floating breakwater using the VOF method is investigated in [12]. The result showed that the transmission coefficient is sensitive, especially in small wave height for regular and random waves. Subsequently, a wing box-type and four typical box-type floating breakwaters have been studied by [13], [14] using SPH numerical simulation. The numerical results show that the protruding plate can reduce wave energy [13]. The floating breakwaters have better performance in the larger and lighter breakwaters and greatly sensitive to the immersion depth [14]. The energy dissipating performances and motion responses of floating breakwaters under regular or irregular waves are investigated using numerical simulation [15]. Under regular waves, the wave transmission (CT) decreases with H/L and B/L when B/L < 0.35, while under irregular waves observed the negative correlation between pitch motion and wave transmission. Also, numerical simulations of three kinds of floating breakwaters are examined in regular waves to compare the performance by [16].

Furthermore, based on the previous studies, there is no investigation regarding the optimal transmission coefficient of floating breakwater using a basic geometric shape applied to the floating breakwater's front side to reduce wave energy. They only examined the basic geometry as the floating breakwater body, not used to the front side (porous). Whereas, based on previous research, porous breakwaters are very effective in reducing the transmission coefficient.

This study aims to develop floating breakwater models by optimizing the wave transmission coefficient (CT) due to the wave force. The study is expected to contribute to the development of ocean floating breakwater in Indonesia's coastline. In this analysis, a numerical study is calculated by CFD based on the VOF method using Flow 3D Software. The basic model (regular ponton (RG) floating breakwater) is modified into several notched shapes. Three floating breakwater models, such as square notch (SQ), circular notch (CN), and triangular notch (VN), were developed. Data parameters and numerical models were validated by the result of experiments conducted by [2]. The CFD model development will be explained in detail in the next section.

2. Materials and Methods

2.1. Floating Breakwater Simulation

Floating breakwater geometry was based on the regular pontoon experiment test [2]. The experiment conducted a two-dimensional physical model test where cross-sections were tested and analyzed in the wave flume. The data parameter of regular pontons is shown in Table 1, and the basic cross-section of the regular pontoon is illustrated in Figure 1. Furthermore, the experimental model will be developed on a porous shape on the side plates with numerical simulations using CFD to optimize wave transmission. The variation of the developed model floating breakwater can be seen in Figure 2.

Table 1. Regular pontoon dimensions

No	Geometry	Dimension [m]
1	Length (*L*)	0.58
2	Width (*W*)	0.46
3	Draft (*D*)	0.31
4	Height (*H*)	0.39

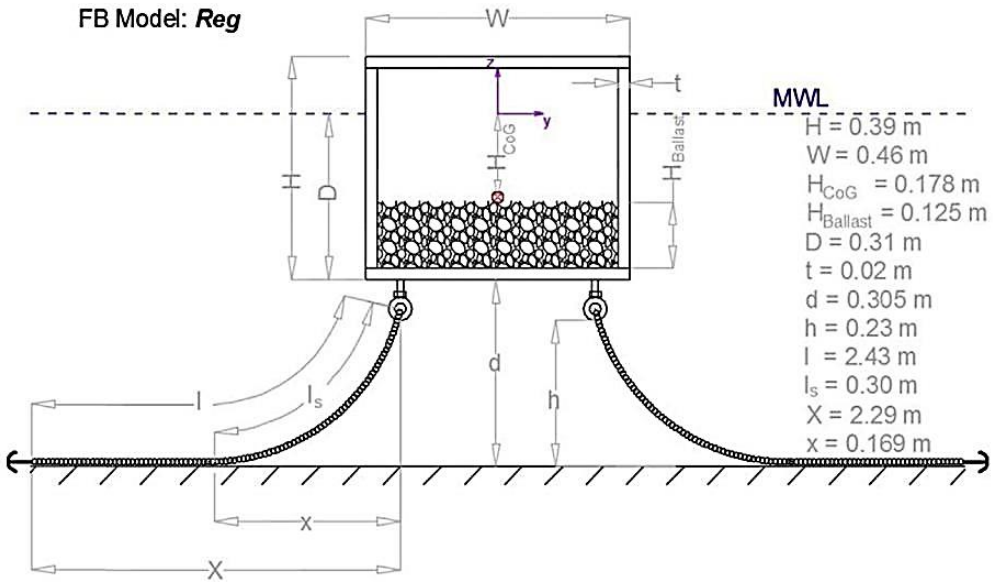

Figure 1. Basic Cross-Section Regular Pontoon Floating Breakwater

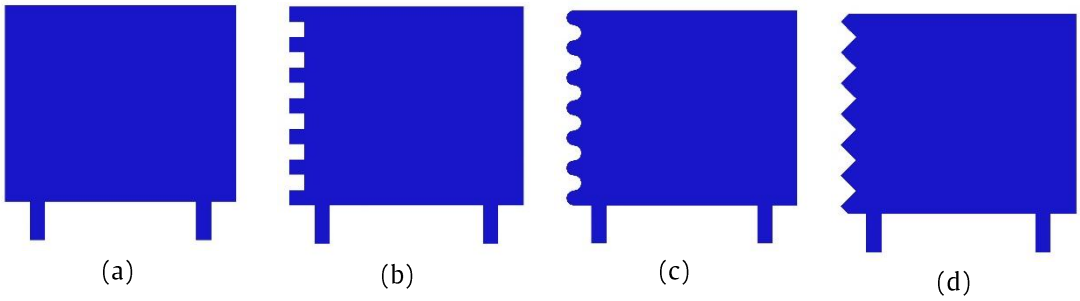

Figure 2. Developed Notched Shape of Floating Breakwater a) Regular Pontoon, b) Square Notch, c) Circular Notch, d) Triangular Notch

Table 2. Parameter wave data

No	Wave length L [m]	Wave period T [s]	Frequency f [Hz]	Depth ratio h/L	Wave height $H_{(2\%)}$	X-axis Figure 4 d/gT^2	Y-axis Figure 4 H/gT^2
1	1.174	0.868	1.152	0.524	0.023	0.083	0.0031
2	1.883	1.116	0.896	0.327	0.036	0.050	0.0029
3	2.252	1.240	0.806	0.273	0.041	0.040	0.0027
5	3.333	1.613	0.620	0.185	0.052	0.024	0.0020
6	4.024	1.861	0.538	0.153	0.055	0.018	0.0016

2.2. Data Parameter

The data were composed of wave parameters that were scaled using Froude scaling by 1:65. Froude scaling was considered valid as long as viscous effects are negligible. The 2nd stokes wave was used in this simulation because the relationship between $\frac{d}{gT^2}$ vs $\frac{H}{gT^2}$ (see Table 2) gets the 2nd order stokes area in the wave theory (see Figure 4). Table 2 shows the condition of the wave data parameter for numerical simulations.

2.3. Wave Flume

The flume dimensions are 28 m in length, 0.6 m in width, 0.8 m in height, and 0.615 m in the initial surface elevation. The flume was filled with fresh water with a density of 1000 kg/m^3. The flume was equipped with a wavemaker at one side and a wave absorber at the other side. The floating breakwaters were placed almost cover the entire width of the flume to reduce the sidewalls' effect. The illustration of the wave flume can be seen in Figure 6.

2.4. Wave Measurement and Analysis

The motion response of floating breakwaters is not described in six degrees of freedom (DOF). The objective of this study is to obtain the transmission coefficient (CT), the ratio of transmitted wave height (HT) to incident wave height (Hi). The transmission coefficient can be shown in Eq. 1 as follow:

$$C_T = H_T/H_i \quad (1)$$

Measurement of transmitted and incident wave heights was represented by surface elevation using wave gauges. A total of four-wave gauges were placed on the incident side, while three-wave gauges were placed on the left side, as illustrated in Figure 7.

2.5. Mooring System

The mooring lines were installed only to keep floating breakwater in the position. The mooring system affected the stability performances and the mooring forces. There were four mooring lines on each corner of the floating breakwater and two other on each cross-section side. The submerged of the mooring line has a weight w = 0.589 N/m. The mooring line was made from polyethylene (PE) with a density (ρ) of 880 kg/m^3 with a diameter of 0.01 m. The whole dimensions of the mooring line are illustrated in Figure 1.

2.6. Stokes Wave Theory

The 2nd order Stokes wave can be generated at a mesh boundary. The 2nd order Stokes wave theory is used to simulate the model developed by Fenton [17]. The Stokes wave theory is a nonlinear wave with higher wave amplitude than the Airy wave theory. Figure 3 described the stokes wave entering the left side of the computational domain where the wave train is assumed to come from the flat bottom reservoir to the computational domain by crossing the mesh boundary. The free surface elevation η (x,t), and the velocity in x and z directions $u(x,z,t)$ and $w(x,z,t)$ of the 2nd order stokes wave theory is as follow:

$$\eta(x,t) = d + \frac{\varepsilon}{k}\cos kX + \frac{\varepsilon^2}{k}B_{31}(\cos kX - \cos 3kX) \quad (2)$$

$$u(x,z,t) = U + C_0(\frac{g}{k^3})^{1/2}\sum_{i=1}^{2}\varepsilon^i\sum_{j=1}^{i}A_{ij}jk\cosh jkz\cos jkX \quad (3)$$

$$w(x,z,t) = C_0(\frac{g}{k^3})^{1/2}\sum_{i=1}^{2}\varepsilon^i\sum_{j=1}^{i}A_{ij}jk\sinh jkz\sin jkX \quad (4)$$

Where $\varepsilon = \frac{kH}{2}$ also known as wave steepness, X=x-ct, and kX=kx-ωt, k is the wave number, and ω is the angular frequency. The coefficient A_(i,j), B_(i,j), and C_0 are nonlinear functions of kd and are presented in [18]. Figure 4 shows the selection of wave theory based on the dimensionless ratio of $\frac{d}{gT^2}$ and $\frac{H}{gT^2}$.

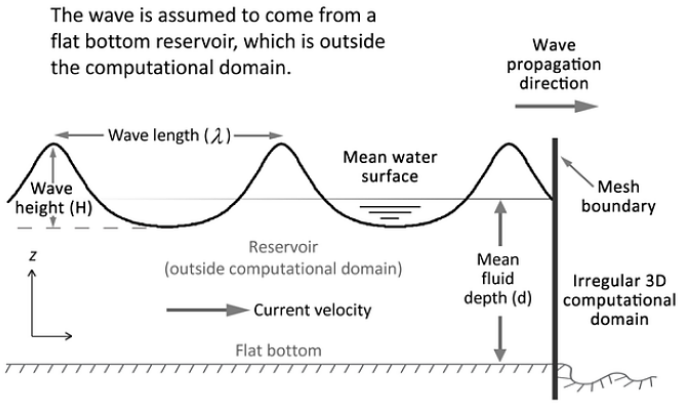

Figure 3. The Stokes wave entering the computational domain [17]

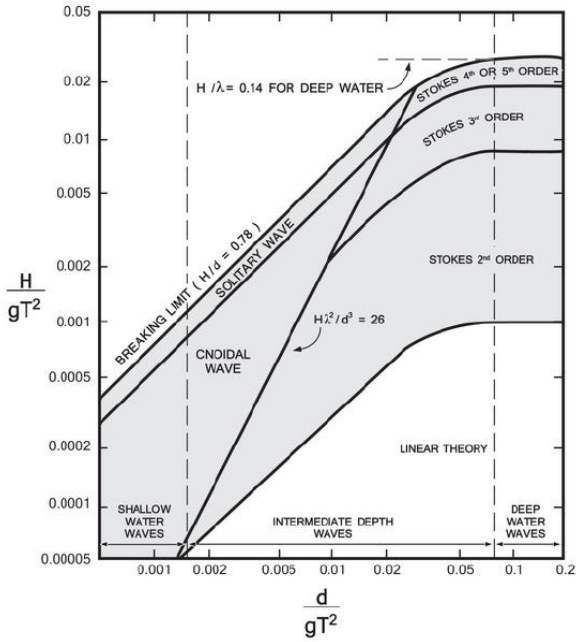

Figure 4. Various wave theory [19]

2.7. CFD Modelling

In this research, CFD modeling has been used using Flow 3D software. In Flow 3D, the fluid flow environment is limited by boundary conditions to simulate the particular investigation area's surrounding effects. The principle of Flow 3D described the behavior of fluid flow in which the equation of fluid motion was solved by RANS (Reynolds Averaged Navier-Stokes) equation, as shown in Eq. 5. The solution of the equation of motion of fluid flow for control volume was carried out on a staggered and structured finite-difference grid [12]. The simulation was conducted by preparing a computational grid in Flow 3D using a rectangular grid. The free surface was tracked by combining the VOF method with the Reynolds Averaged Navier-Stokes (RANS) equation. In the computation of turbulence flows, Renormalization-Group (RNG) turbulence was used because it has a low Reynold number effect [19] and has the most accurate for the best real-world problems [17]. The RNG group model uses equations similar to the equations for the k-e model. This approach applied statistical methods to derivate

the average equations for turbulence quantities, such as turbulent kinetic energy and dissipation rate. Generally, the RNG group model has wider applicability than the standard k-e model [17].

The equations of motion for the fluid velocity components (u, v, w) in the three coordinate directions are the Navier-Stokes equations with some additional terms. The equation is as follow:

$$\frac{\partial u}{\partial t}+\frac{1}{V_F}\left\{uA_x\frac{\partial u}{\partial x}+vA_yR\frac{\partial u}{\partial y}+wA_z\frac{\partial u}{\partial z}\right\}-\xi\frac{A_yv^2}{xV_F}=-\frac{1}{\rho}\frac{\delta p}{\delta x}+G_x+f_x-b_x-\frac{R_{SOR}}{\rho V_F}(u-u_w-\delta u_s)$$
$$\frac{\partial v}{\partial t}+\frac{1}{V_F}\left\{uA_x\frac{\partial v}{\partial x}+vA_yR\frac{\partial v}{\partial y}+wA_z\frac{\partial v}{\partial z}\right\}+\xi\frac{A_yuv}{xV_F}=-\frac{1}{\rho}\frac{\delta p}{\delta y}+G_y+f_y-b_y-\frac{R_{SOR}}{\rho V_F}(v-v_w-\delta v_s) \quad (5)$$
$$\frac{\partial w}{\partial t}+\frac{1}{V_F}\left\{uA_x\frac{\partial w}{\partial x}+vA_yR\frac{\partial w}{\partial y}+wA_z\frac{\partial w}{\partial z}\right\}=-\frac{1}{\rho}\frac{\delta p}{\delta z}+G_z+f_z-b_z-\frac{R_{SOR}}{\rho V_F}(w-w_w-\delta w_s)$$

Where (G_x, G_y, G_z) are body accelerations, (f_x, f_y, f_z) are viscous accelerations, and (b_x, b_y, b_z) are flow losses in porous media or across porous baffle plates, and the final terms account for the injection of mass at a source represented by a geometry component

2.8. Boundary Condition

The simulation was used by Flow-3D software. The simulation was firstly conducted by modeling the floating breakwater geometry in the stereolithographic format (.stl format). Then, the .stl file format was imported into the Flow-3D software. Then, the computational domain wave flume as a boundary condition set was arranged. The boundary condition was used to assume the solution at the boundaries (boundary condition setting) and initial time (initial conditions) and also to use these values to solve the partial differential equation (PDE) governing in the domain [17]. The purpose of boundary conditions was to determine model conditions that represented the experimental condition. The view of the model can be seen in Figure 5. Boundary conditions used in the model are as follow:

(1) Wave: A wave boundary condition was defined at left (X Min). A surface wave entered the computational domain and propagated in the direction normal to the boundary. The wave was set 2nd stokes as wave generator represent the physical wave conditions at the boundary.
(2) Outflow: The outflow boundary condition was defined at right (X Max). It allowed users to investigate the effects of wave interactions with structures numerically. The capability permitted a reduction in the extent of the computing mesh needed for accurate computations. A wave-absorbing layer was used to reduce the reflection of the periodic wave at an open boundary.
(3) Symmetry: The symmetry condition was defined at the front (Y Min), behind (Y Max), below (Z Min), and up (Z Max). No-slip conditions were imposed using the wall shear-stress options described in the Prandtl Mixing Length model. The symmetry condition can be specified as free-slip conditions that have a non-zero wall shear-stress.

2.9. Meshing

Mesh block was used to determine the modeled area. The smaller mesh will be more detailed, but the output files will be larger, and the simulation run longer. Floating breakwater modeling used one mesh block with a meshing size of 0.04 m at a total length (X-axis) of 28 m, total width (Y-axis) of 0.6 m, and total height (Z-axis) of 0.8 m. See Figure 8 for detail meshing.

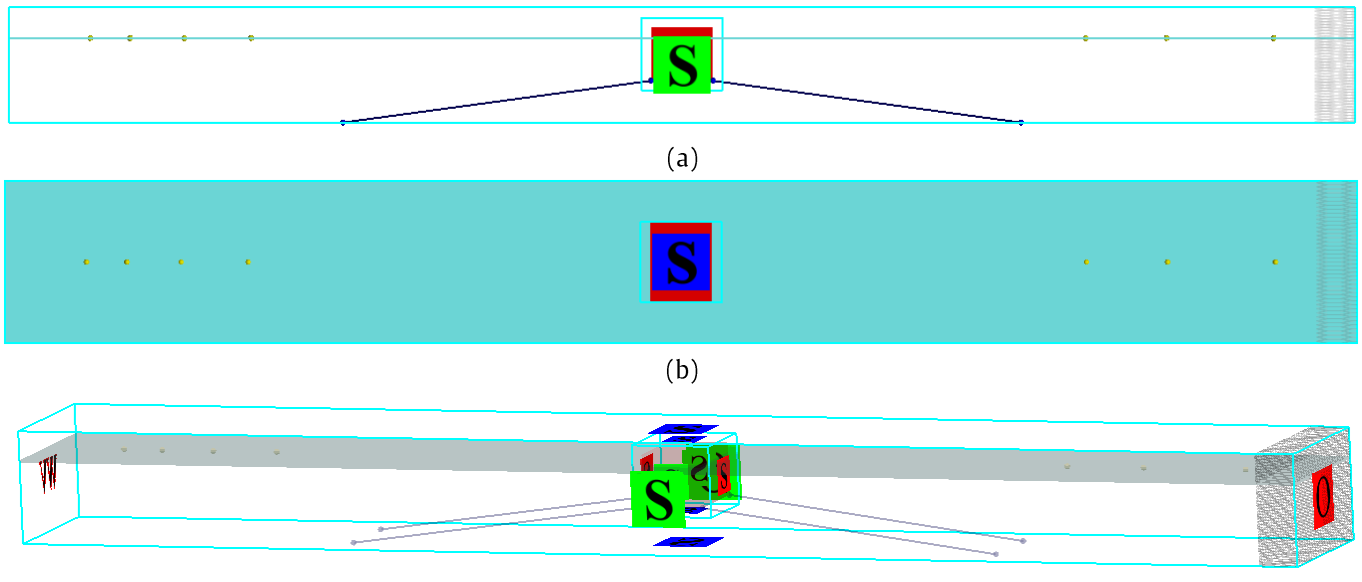

Figure 5. (a) Side View, (b) Top View, (c) Isometric View

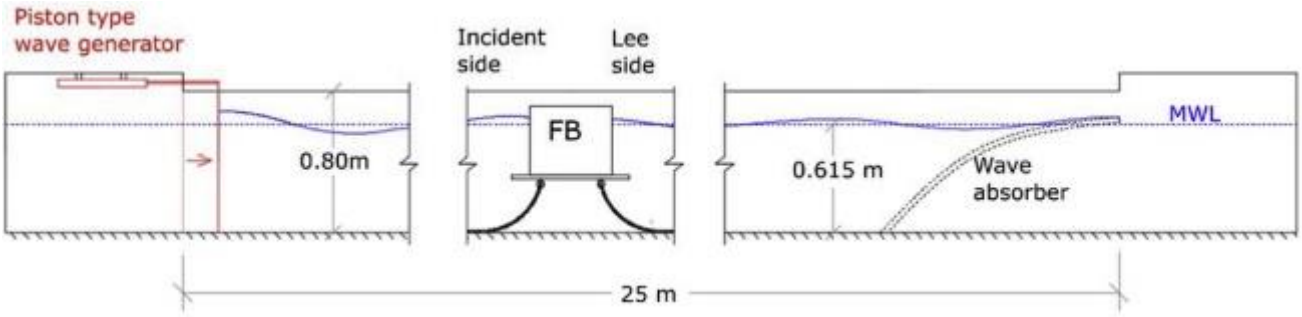

Figure 6. Sketch of The Wave Flume

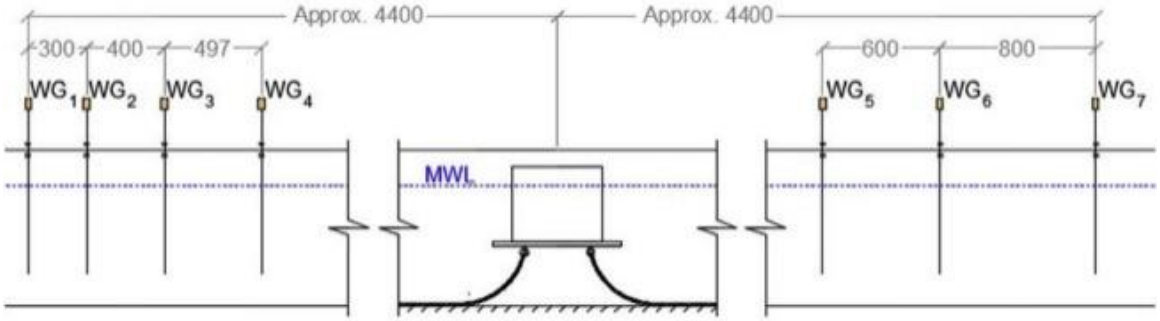

Figure 7. Position Wave Gauges in The Unit [mm]

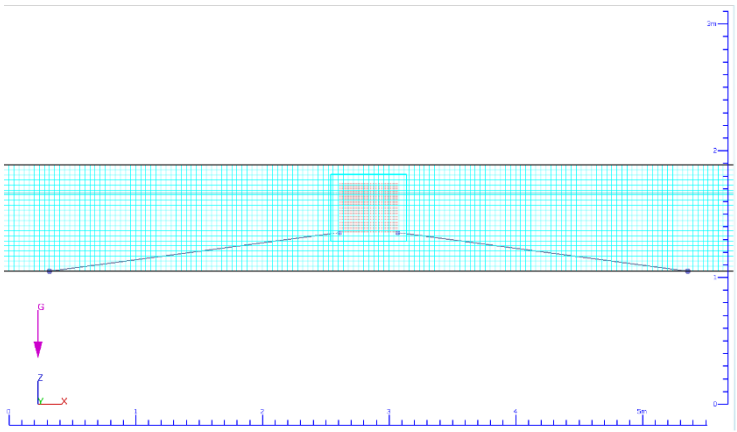

(a)

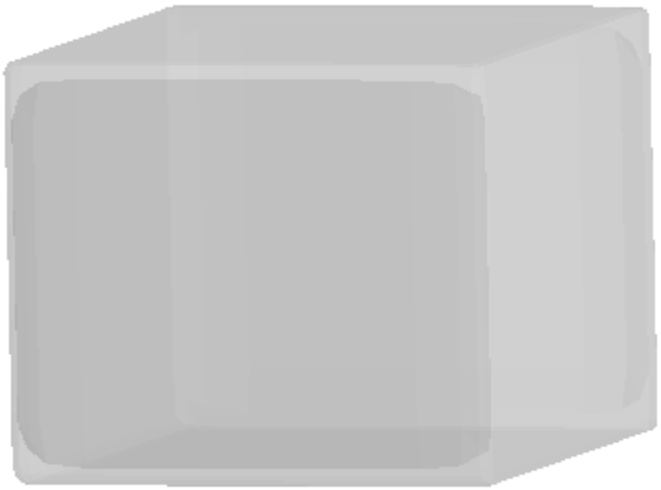

(b)

Figure 8. (a) Grid of the Model, (b) Rendering of the Model

3. Results and Discussion

3.1. Model validation

Validation was conducted by comparing the experimental results of the transmission coefficient by [2] with the numerical study of the CFD aided with Flow 3D Software. Christensen has surveyed three floating breakwater shapes, but only one Regular Pontoon (RG) was validated in this study. The purpose of validation was to find out whether the numerical analysis was suitable for the experimental result. Further, when the verification was conducted, the model's development can be explored for other optimal shapes.

In this study, validation is conducted based on comparing the transmission coefficient between numerical test and experimental test. The error rate refers to the Mean Absolute Percentage Error (MAPE) theory [20]. The MAPE theory can be seen in detail in Table 3. The validation results can be seen in Figure 10 and Table 4. Based on the MAPE theory, this study can be validated with good agreement because the error rate between CT of experiment and CT of numeric is still below 10%. Therefore, it can be developed with more optimal shapes.

Regular Pontoon (RG) is one type of floating breakwater that was examined by [2] and validated with a numerical model. Figure 9 is the shape of the wave profile and the distribution of the current velocity through the structure in one wave variation with time series. The reduction in wave height at the rear of the structure can be seen with the transmission wave profile that is more gentle than the incident waves. A decrease follows the decrease in wave height in the current velocity, which is indicated by the change in the velocity contour's gradation. When the waves are higher and directly in front of the structure, the current tends to be faster. When the waves are lower and behind the structure, the current speed tends to be slower. Both of these can be seen by changing the current velocity contours. Therefore, the fluid flow velocity is also affected by a structure's presence and directly proportional to the wave height. The velocity pattern can be seen Figure 9, and the validation of the transmission coefficient of numerical simulation results can be seen in Table 4.

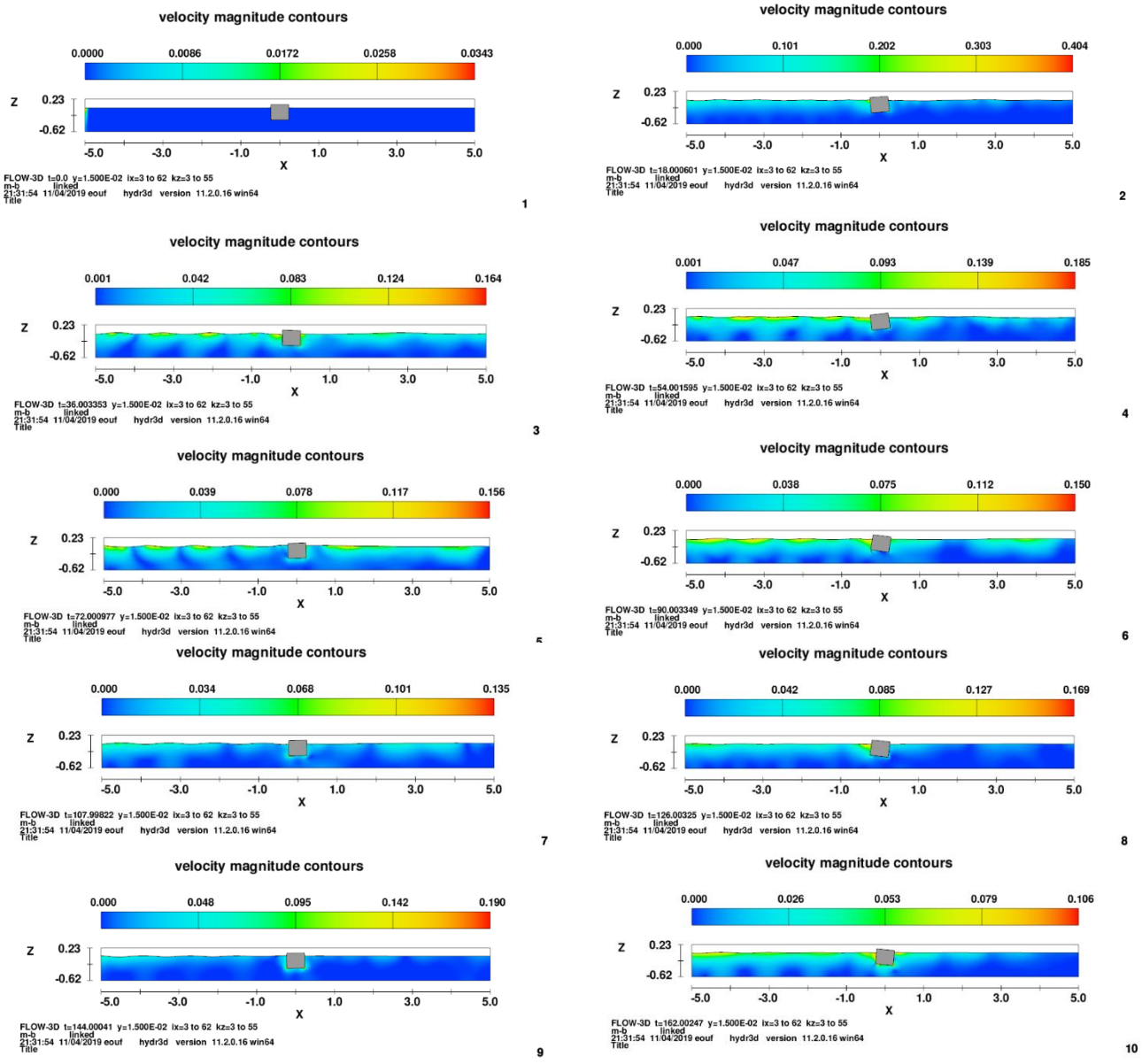

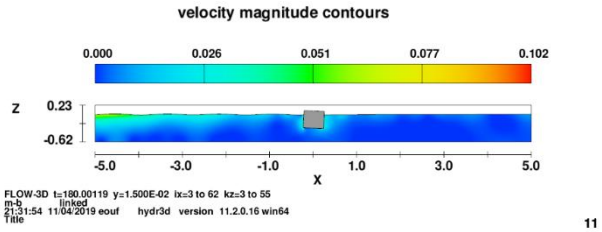

Figure 9. Characteristics of velocity patterns on regular pontoon (RG) floating breakwater

The transmission coefficient is obtained from the analysis of the output surface elevation results in Flow 3D software, as shown in Figure 10. Surface elevation data used to analyze the transmission coefficient are obtained from wave gauge 1 (in front of the structure) and wave gauge 5 (behind the structure). Surface elevation data is converted into wave height using Wave Analysis (WAVAN) coding. Then, to get the transmission coefficient, the calculation is according to Eq. 1. The results of regular pontoon coefficient transmission are shown in Table 4.

3.2. Transmission Coefficient Development Notched Shape

The wave transmission coefficient (CT) due to the wave force to the structure is estimated. There are several factors that influence it; one of them is wave steepness (H/gT^2). The modeling results obtained free surface elevation data for each wave observation point and velocity magnitude data for each current velocity observation point.

The wave data used in the transmission coefficient (CT) analysis is based on the processed free surface elevation data for all predetermined observation points. The data obtained is in water level vs. time series data in meters and seconds. The wave data is then analyzed with WAVAN coding to determine the average period (T) and average wave height (H) for each observation point. This is done for the wave observation points at the front and back of the structure. The wave height in front of and behind the structure is then used to determine the transmission coefficient (CT), which is represented by CT on X-axis and the wave steepness (H/gT^2) in Y-axis

There are three notched shapes of the floating breakwater, as illustrated in Figure 2. In this analysis, Flow 3D software is used to obtain the transmission coefficient of Regular Pontoon. The results of coefficient transmission of three different notched shapes are shown in Table 5. The average value of the transmission coefficient each of 0.6248, 0.6886, and 0.6735. The smaller the transmission coefficient value, the more optimal. It can be summarized that the square notch (SQ) model is the most optimal floating breakwater structure.

Table 3. MAPE Theory

No	MAPE Value	Prediction
1	MAPE ≤ 10%	High
2	10% <MAPE ≤ 20%	Good
3	20%< MAPE ≤ 50%	Reasonable
4	MAPE >50%	Low

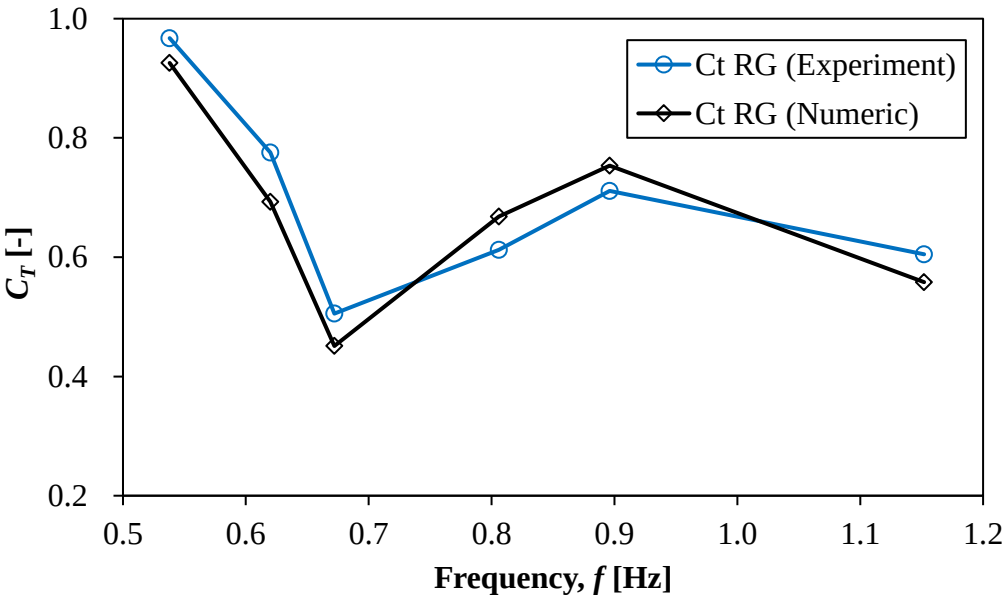

Figure 10. Validation results

Table 4. Value of Validation Results

No	Data Input H[m]	T[s]	H_I	H_T	C_T Experimental	C_T Numerical	Error (%)
1	0.0230	0.8680	0.0353	0.0197	0.6046	0.5581	8.3370
2	0.0360	1.1160	0.0329	0.0248	0.7114	0.7538	5.6248
3	0.0410	1.2400	0.0491	0.0328	0.6125	0.6680	8.3117
4	0.0490	1.4880	0.0521	0.0235	0.5054	0.4511	12.0483
5	0.0520	1.6130	0.0589	0.0408	0.7756	0.6927	11.9677
6	0.0550	1.8610	0.0498	0.0461	0.9673	0.9257	4.4936
	Mean Absolute Percentage Error (MAPE)						8.4638

Table 5. The Transmission Coefficient Of Notched Shape

H/gT^2 [-]	Transmission Coefficient (C_T) Model RG	Model SQ	Model CN	Model VN
0.0031	0.5581	0.4000	0.5076	0.4963
0.0029	0.7538	0.7222	0.7588	0.7515
0.0027	0.6680	0.5706	0.5963	0.5779
0.0023	0.4511	0.6250	0.7215	0.7040
0.0020	0.6927	0.6494	0.7534	0.6998
0.0016	0.9257	0.7818	0.7766	0.8114
Average of C_T [-]	0.6749	0.6248	0.6886	0.6735

4. Conclusion

The study presents a numerical analysis to analyze optimum transmission coefficients of three different notched models of the floating breakwater. Numerical simulation was validated with the experimental test. The result shows lower limits of error with an error rate of 8.5%. So, it can be developed for more optimum notched shape models. Some models are overestimated, which may be common as a numerical approach and can be tolerated. It is a high prediction approaching experimental trial results.

Simulation results show the transmission coefficient created by the wave parameters, specifically wave period and high wave. To minimize the value of the transmission coefficient, it can use the developed notched model in front of the floating breakwater structure. Three development models: square notch (SQ), circular notch (CN), and triangular notch (VN), have an average transmission coefficient of 0.6248, 0.6886, and 0.6735, respectively. It can be summarized that the smaller the transmission coefficient value, the more optimal the model. The square notch (SQ) model is the most optimal floating breakwater structure.

Based on the research results, the square notch (SQ) model is the most optimal floating breakwater in reducing wave energy. The experimental study can be carried out using the square notch (SQ) model as the optimum breakwater notch shape in further research. The square notch (SQ) model's motion can be analyzed and compared with a numerical approach.

References

[1] J. Dai, C. M. Wang, T. Utsunomiya, and W. Duan, "Review of recent research and developments on floating breakwaters," *Ocean Engineering*, vol. 158, pp. 132–151, 2018. doi: 10.1016/j.oceaneng.2018.03.083

[2] A. C. Biesheuvel, 2013. *Effectiveness of Floating Breakwaters: wave attenuating floating structures.* Master of Science Thesis. Delft University of Technology: Netherlands.

[3] C. Y. Ji, X. Q. Bian, Y. Cheng, and K. Yang, "Experimental study of hydrodynamic performance for double-row rectangular floating breakwaters with porous plates," *Ships Offshore Structures*, vol. 14, no. 7, pp. 737–746, 2019. doi: 10.1080/17445302.2018.1558521

[4] E. D. Christensen, H. B. Bingham, A. P. Skou Friis, A. K. Larsen, and K. L. Jensen, "An experimental and numerical study of floating breakwaters," *Coastal Engineering*, vol. 137, pp. 43–58, 2018., doi: 10.1016/j.coastaleng.2018.03.002

[5] I. H. Cho, "Transmission coefficients of a floating rectangular breakwater with porous side plates," *International Journal of Naval Architecture and Ocean Engineering*, vol. 8, no. 1, pp. 53–65, 2016. doi: 10.1016/j.ijnaoe.2015.10.002

[6] H. Y. Wang and Z. C. Sun, "Experimental study of a porous floating breakwater," *Ocean Engineering*, vol. 37, pp. 520–527, 2010. doi: 10.1016/j.oceaneng.2009.12.005

[7] C-Y. Ji, X. Chen, J. Cui, Z-M. Yuan, A. Incecik, "Experimental Study of a New Type of Floating Breakwater," *Ocean Engineering*, Vol. 105, pp. 295–303, 2015. doi: 10.1016/j.oceaneng.2015.06.046

[8] C-Y. Ji, Y-C. GUO, J. Cui, Z-M. Yuan, X-J. Ma. "3D experimental study on a cylindrical floating breakwater system," *Ocean Engineering*, Vol. 125, pp. 38-50, 2016. doi: 10.1016/j.oceaneng.2016.07.051

[9] C-Y. Ji, Y. Cheng, K. Yang, G. Oleg, "Numerical and experimental investigation of hydrodynamic performance of cylindrical dual pontoon-net floating breakwater." *Coastal Engineering*. Vol. 129, pp. 1-16, 2017. doi: 10.1016/j.coastaleng.2017.08.013

[10] M. A. Rahman, N. Mizutani, and K. Kawasaki, "Numerical modeling of dynamic responses and mooring forces of submerged floating breakwater," *Coastal Engineering*, vol. 53, no. 10, pp. 799–815, 2006, doi: 10.1016/j.coastaleng.2006.04.001

[11] X. Liu, Y. Liu, P. Lin, A-J. Li, "Numerical simulation of wave overtopping above perforated caisson breakwaters," *Coastal*

Engineering, vol. 163, 2021. doi: 10.1016/j.coastaleng.2020.103795
[12] S. F. Abdullah, A. Fitriadhy, M. Hairil, and A. Jusoh, "Hydrodynamic performance of cylindrical floating breakwater in waves," *International Journal of Automotive and Mechanical Engineering*, vol. 14, no. 4, pp. 4715–4729, 2017, doi: 10.15282/ijame.14.4.2017.10.0371
[13] Z. Liu, Y. Wang, W. Wang, X. Hua, "Numerical modelling and optimization of a winged box-type floating breakwater by Smoothed Particle Hydrodynamics," *Coastal Engineering,* vol. 188, 2019. doi: 10.1016/j.oceaneng.2019.106246
[14] Z. Liu, Y. Wang, "Numerical investigations and optimizations of typical submerged box-type floating breakwaters using SPH," *Ocean Engineering,* vol. 209, 2020, doi: 10.1016/j.oceaneng.2020.107475
[15] J. M. Zhan, X-B. Chen, Y-J. Gong, W-Q. Hu, "Numerical investigation of the interaction between an inverse T-type fixed/floating breakwater and regular/irregular waves," *Ocean Engineering,* vol. 137, pp. 110-119, 2017. doi: 10.1016/j.oceaneng.2017.03.058
[16] K-L. Jeong, Y-G. Lee, "Numerical simulations of two-dimensional floating breakwaters in regular waves using fixed cartesian grid," *International Journal of Naval Architecture and Ocean Engineering*, vol. 6, no. 2, pp. 206-218, 2014 doi: 10.2478/IJNAOE-2013-0173
[17] I. Flow Science, "FLOW-3D Documentation v11." p. 330, 2014.
[18] U.S. Army Corps of Engineers, *Coastal Engineering Manual*, In 6 Volum. Washington D.C, 2006.
[19] N. Koutsourakis, J. G. Bartzis, N. C. Markatos, "Evaluation of Reynolds stress, k-ε and RNG k-ε turbulence models in street canyon flows using various experimental datasets," *Environmental Fluid Mechanics*, vol. 12, pp. 379–403, 2012. doi: 10.1007/s10652-012-9240-9
[20] S. Kim, H. Kim, "A new metric of absolute percentage error for intermittent demand forecast," *International Journal of Forecasting*, vol. 32, no. 3, pp. 669-679, 2016. doi: 10.1016/j.ijforecast.2015.12.003